Photo-induced handedness inversion with opposite-handed cholesteric liquid crystal

Yun-Han Lee,[1] Ling Wang,[2] Huai Yang,[2] and Shin-Tson Wu[1*]

[1]*CREOL, The College of Optics and Photonics, University of Central Florida, Orlando, Florida 32816, USA*
[2]*Department of Materials Science and Engineering, Peking University, Beijing 100871, China*
**swu@ucf.edu*

Abstract: Cholesteric liquid crystals (CLCs) are self-organized helical nano-structures that selectively reflect certain wavelength of a circularly polarized light. For most CLCs, the handedness is fixed once a chiral dopant is employed. Here, we report a handedness-invertible CLC through opposite-handed doping of a photo-sensitive chiral azobenzene dopant and a photo-stable chiral dopant. With high solubility of the photo-sensitive chiral dopant, the Bragg reflection can be tailored from right-handed to left-handed upon UV exposure. The reversed process can be easily carried out through heating.

OCIS codes: (160.3710) Liquid crystals; (230.3720) Liquid-crystal devices; (230.1480) Bragg reflectors; (160.1585) Chiral media.

References and links

1. P. G. de Gennes and J. Prost, *The Physics of Liquid Crystals* (Oxford, 1995).
2. S.-T. Wu and D.-K. Yang, *Reflective Liquid Crystal Displays* (Wiley, 2001).
3. V. Vinvogradova, A. Khizhnyaka, L. Kutulyaa, Yu. Reznikova, and V. Resihetnyaka, "Photoinduced charge of cholesteric LC-pitch," Mol. Cryst. Liq. Cryst. (Phila. Pa.) **192**(1), 273–278 (1990).
4. B. L. Feringa, W. F. Jager, B. de Lange, and E. W. Meijer, "Chiroptical molecular switch," J. Am. Chem. Soc. **113**(14), 5468–5470 (1991).
5. B. L. Feringa, N. P. M. Huck, and H. A. van Doren, "Chiroptical switching between liquid crystalline phases," J. Am. Chem. Soc. **117**(39), 9929–9930 (1995).
6. U. A. Hrozhyk, S. V. Serak, N. V. Tabiryan, and T. J. Bunning, "Phototunable reflection notches of cholesteric liquid crystals," J. Appl. Phys. **104**(6), 063102 (2008).
7. T. V. Mykytiuk, I. P. Ilchishin, O. V. Yaroshchuk, R. M. Kravchuk, Y. Li, and Q. Li, "Rapid reversible phototuning of lasing frequency in dye-doped cholesteric liquid crystal," Opt. Lett. **39**(22), 6490–6493 (2014).
8. P. Shibaev, R. Sanford, D. Chiappetta, V. Milner, A. Genack, and A. Bobrovsky, "Light controllable tuning and switching of lasing in chiral liquid crystals," Opt. Express **13**(7), 2358–2363 (2005).
9. S. Kurihara, S. Nomiyama, and T. Nonaka, "Photochemical control of the macrostructure of cholesteric liquid crystals by means of photoisomerization of chiral azobenzene molecules," Chem. Mater. **13**(6), 1992–1997 (2001).
10. C.-T. Wang, Y.-C. Wu, and T.-H. Lin, "Photo-switchable bistable twisted nematic liquid crystal optical switch," Opt. Express **21**(4), 4361–4366 (2013).
11. A. Urbas, V. Tondiglia, L. Natarajan, R. Sutherland, H. Yu, J.-H. Li, and T. Bunning, "Optically switchable liquid crystal photonic structures," J. Am. Chem. Soc. **126**(42), 13580–13581 (2004).
12. Y.-G. Fuh, M.-S. Tsai, L.-J. Huang, and T.-C. Liu, "Optically switchable gratings based on polymer-dispersed liquid crystal films doped with a guest–host dye," Appl. Phys. Lett. **74**(18), 2572–2574 (1999).
13. Q. Hong, T. X. Wu, and S. T. Wu, "Optical wave propagation in a cholesteric liquid crystal using the finite element method," Liq. Cryst. **30**(3), 367–375 (2003).
14. Y.-J. Liu, Y.-B. Zheng, J. Shi, H. Huang, T. R. Walker, and T. J. Huang, "Optically switchable gratings based on azo-dye-doped, polymer-dispersed liquid crystals," Opt. Lett. **34**(15), 2351–2353 (2009).
15. I. P. Ilchishin, L. N. Lisetski, and T. V. Mykytiuk, "Reversible phototuning of lasing frequency in dye doped cholesteric liquid crystal and ways to improve it," Opt. Mater. Express **1**(8), 1484–1493 (2011).
16. P. van de Witte, M. Brehmer, and J. Lub, "LCD components obtained by patterning of chiral nematic polymer layers," J. Mater. Chem. **9**(9), 2087–2094 (1999).
17. T. J. White, S. A. Cazzell, A. S. Freer, D.-K. Yang, L. Sukhomlinova, L. Su, T. Kosa, B. Taheri, and T. J. Bunning, "Widely tunable, photoinvertible cholesteric liquid crystals," Adv. Mater. **23**(11), 1389–1392 (2011).
18. N. Katsonis, E. Lacaze, and A. Ferrarini, "Controlling chirality with helix inversion in cholesteric liquid crystals," J. Mater. Chem. **22**(15), 7088–7097 (2012).

#244290 Received 2 Jul 2015; revised 15 Aug 2015; accepted 17 Aug 2015; published 19 Aug 2015

19. M. Mathews and N. Tamaoki, "Reversibly tunable helicity induction and inversion in liquid crystal self-assembly by a planar chiroptic trigger molecule," Chem. Commun. (Camb.) **24**(24), 3609–3611 (2009).
20. M. Mathews, R. S. Zola, S. Hurley, D.-K. Yang, T. J. White, T. J. Bunning, and Q. Li, "Light-driven reversible handedness inversion in self-organized helical superstructures," J. Am. Chem. Soc. **132**(51), 18361–18366 (2010).
21. I. Dierking, F. Gieβelmann, P. Zugenmaier, W. Kuczynskit, S. T. Lagerwall, and B. Stebler, "Investigations of the structure of a cholesteric phase with a temperature induced helix inversion and of the succeeding Sc* phase in thin liquid crystal cells," Liq. Cryst. **13**(1), 45–55 (1992).
22. M. Mitov and N. Dessaud, "Going beyond the reflectance limit of cholesteric liquid crystals," Nat. Mater. **5**(5), 361–364 (2006).
23. I. Gvozdovskyy, O. Yaroshchuk, M. Serbina, and R. Yamaguchi, "Photoinduced helical inversion in cholesteric liquid crystal cells with homeotropic anchoring," Opt. Express **20**(4), 3499–3508 (2012).
24. Q. Li, L. Green, N. Venkataraman, I. Shiyanovskaya, A. Khan, A. Urbas, and J. W. Doane, "Reversible photoswitchable axially chiral dopants with high helical twisting power," J. Am. Chem. Soc. **129**(43), 12908–12909 (2007).
25. Y.-J. Liu, P.-C. Wu, and W. Lee, "Spectral variations in selective reflection in cholesteric liquid crystals containing opposite-handed chiral dopants," Mol. Cryst. Liq. Cryst. (Phila. Pa.) **596**(1), 37–44 (2014).
26. Y. Huang, Y. Zhou, C. Doyle, and S. T. Wu, "Tuning the photonic band gap in cholesteric liquid crystals by temperature-dependent dopant solubility," Opt. Express **14**(3), 1236–1242 (2006).
27. L. Wang, H. Dong, Y. Li, C. Xue, L.-D. Sun, C.-H. Yan, and Q. Li, "Reversible near-infrared light directed reflection in a self-organized helical superstructure loaded with upconversion nanoparticles," J. Am. Chem. Soc. **136**(12), 4480–4483 (2014).
28. I. Dierking, *Textures of Liquid Crystals* (Wiley, 2006).

1. Introduction

In a cholesteric liquid crystal (CLC), the orientation of each layer is self-organized in a planar helical structure [1]. CLC is generally prepared by doping a chiral compound to a nematic LC host, where the chiral dopant induces a helical twist along the optical axis. For a circularly polarized light with the same handedness, such twist creates an effective periodic refraction index change, resulting in a reflection band when the wavelength matches the helical twist period (pitch length). In a uniform CLC cell, pitch length is roughly the same throughout the sample. In this case, the central wavelength of the reflection band can be described by $\lambda_o = nP \cdot cos\theta$, where n is the average of the extraordinary and ordinary refractive indices, P is the pitch length, and θ is the incident angle. At low chiral concentration, P can be approximated as $P = 1/(C_w \cdot \beta)$, where C_w is the weight concentration of the chiral dopant and β is the helical twisting power, which is governed by the chiral dopant structure and the molecular interaction between chiral dopant and nematic LC host. The pitch length can be shortened by increasing the dopant concentration or increasing the helical twisting power. To achieve high reflectance (>90%) for the same-handed circularly polarized light, the cell gap should be larger than $8P$ [2].

In the past two decades, optical tuning of the helical twisting power has been realized [3–8] and wide applications of optically tunable devices such as tunable lasers, gratings and displays have been demonstrated [9–16]. This tuning was done through introducing azobenzene or azoxybenzenes functional group into chiral materials. Upon UV/Vis exposure, they experience *trans*-*cis* isomerization which leads to a structural change and alters its helical twisting power. Typically, under violet or ultraviolet light illumination, azo-chiral isomerizes to *cis*-form, whereas the reverse process, *cis*-to-*trans* isomerization, can occur thermally or photochemically with the irradiation of a visible light. It is noteworthy that the helical twisting power of the chiral azobenzene dopant exhibits distinct variation between its two states. The change in helical twisting power manifests itself as a change in the wavelength shift of reflection band. With the advanced molecular engineering, the tuning range can be as wide as 2000 nm [17], while the tuning time is normally around a few seconds to few minutes.

Despite the versatility, chirality inversion remains a challenging task [18]. During the past decades, extensive efforts have been made mainly through tailoring the chemical structure such that the helicity inverts upon the exposure to light [19, 20] or heat [21, 22]. They either

#244290 Received 2 Jul 2015; revised 15 Aug 2015; accepted 17 Aug 2015; published 19 Aug 2015

require sophisticated molecular engineering or have limited tenability, and are often encountered by chance. Notably, in a relatively recent work, Gvozdovskyy et al. [23] demonstrated that through doping of different handedness chiral materials, one can obtain CLC with different handedness. This eliminates the need of complicated design of molecular structure. However, due to the limited solubility, the pitch length was much longer than needed to induce chirality inverted Bragg reflection, and only fingerprint textures was observed.

In this paper, with a highly soluble photo-sensitive chiral dopant, we report handedness inversion in a selective Bragg reflection through opposite-handed chiral doping. With high chirality and effective twisting power, we are able to tune the reflection band to near-infrared region and tailor the reflection to longer wavelength and eventually invert the chirality, resulting in opposite-handed infrared reflection through UV exposure. We also studied and formulated the band-shifting behavior and demonstrated a patterned opposite-handed cholesteric reflection.

2. Experimental

A high birefringence nematic LC host BL038 (Merck, n_e = 1.78 and n_o = 1.52 at λ = 633 nm) was used in this experiment in order to obtain high reflectance. In the first part of the experiment, we doped various concentration of a photo-sensitive chiral azobenzene compound PSC-01 (right-handed material with helical twisting power in BL-038 being 64.18 and 16.31 μm^{-1} for its initial state and post-exposure state, respectively; synthesized at PKU following the procedures reported in [24]) to determine the solubility. In the second part, we doped 1.8wt% of a photo-stable chiral compound S-5011 (HCCH, left-handed material with helical twisting power in BL-038 being 103.8 μm^{-1}) and 4.75wt% of PSC-01 to obtain helix inversion in selective reflection band. The chemical structure of PSC-01 is shown in Fig. 1. The cell gap was controlled at 5.2 μm by spacer balls to ensure well-defined helix structure. We then measured the Bragg reflection spectra with an FTIR Spectrometer (PerkinElmer Spectrum Two). The UV exposure was performed with a Mercury lamp (Hamamatsu L8868-01) and its intensity controlled in the 8–16 mW/cm^2 range.

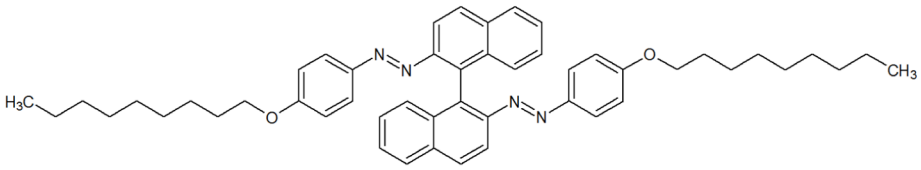

Fig. 1. The chemical structure of PSC-01. The azobenzene bonds are sensitive to UV exposure and they can experience *trans-cis* isomerization which affects the helical twisting power.

3. Results and discussion

First, we measured the solubility of PSC-01 in BL-038 through Bragg reflection. Due to the high twisting power of *trans*-PSC-01, at higher concentration, the reflection band occurs in the UV region and is outside of our detection range. Therefore, we measured the behavior in its post-exposure form where most of the chiral molecules are in *cis*-form and the reflection band lies in infrared region. Note that only PSC-01 was doped and the samples were exposed to 12.4-mW/cm^2 UV light until most PSC-01 was isomerized to the *cis*-form and the reflection band stopped red-shifting. As Fig. 2 depicts, in the low concentration region the reflection wavelength agrees well with that calculated (red curve) with Eq. (1) [2]:

$$\lambda_0 = n / \beta_c C_c, \tag{1}$$

where n (= 1.65) is the average refractive index of BL-038, β_c (= 16.31 μm^{-1}) is the helical twisting power of *cis*-PSC-01, and C_c denotes the concentration of *cis*-PSC-01. As the

#244290 Received 2 Jul 2015; revised 15 Aug 2015; accepted 17 Aug 2015; published 19 Aug 2015

concentration increases, the reflection wavelength gets shorter and then gradually deviates from Eq. (1). Beyond ~10 wt%, the system reaches saturation; further increasing the concentration of PSC-01 does not lead to a significant change in central reflection wavelength. This indicates that the solubility of PSC-01 is limited to ~8 wt%. To keep away from the saturation region, we chose to use 4.75-wt% PSC-01 and 1.8-wt% S-5011 to obtain handedness inversion in the following experiments.

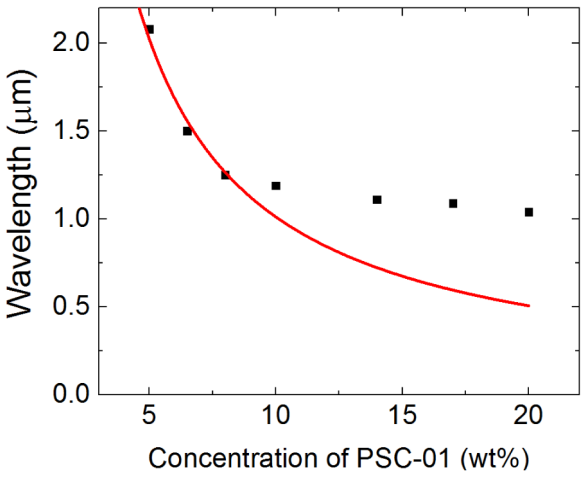

Fig. 2. Measured and calculated reflection wavelength vs. PSC-01 concentration. Dots are measured data and red line represents fitting with Eq. (1). LC host: BL-038.

Figure 3 depicts the handedness inversion mechanisms. When PSC-01 (right-handed; photo-sensitive) and S-5011 (left-handed; photo-stable) are both present, initially the concentration is chosen such that the *trans*-PSC-01 surpasses S-5011 in overall twisting power and a right-handed helix is formed as shown in Fig. 3(a). Upon UV exposure, in Fig. 3(b), *trans*-PSC-01 gradually turns into *cis*-PSC-01 with a reduced helical twisting power so that unwinding occurs. Further, when the effective twisting power of PSC-01 gets weaker than that of S-5011, the handedness is inverted and LCs start to wind in the opposite way, as shown in Fig. 3(c). Finally, in Fig. 3(d), the whole system is dominated by S-5011 and the helix reaches an equilibrium. The reversal process can be carried out either by green light exposure or by heat. The sample can also recover by itself in dark ambient but the required time is much longer.

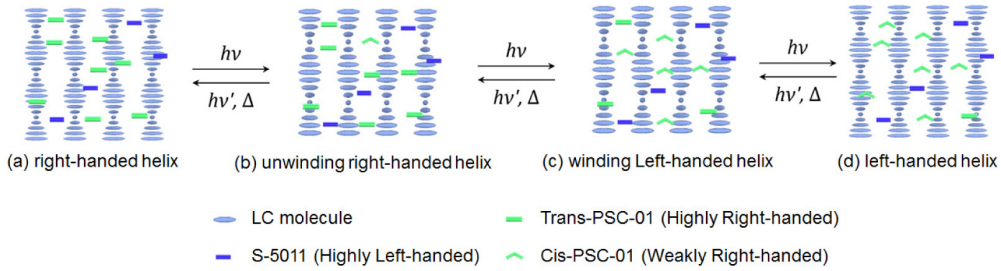

Fig. 3. Mechanisms of opposite-handed cholesteric helix inversion.

Figure 4 shows the measured reflection spectra at different UV-exposure time. Since both dynamic flow and reflection band tuning occur simultaneously, after each UV exposure we waited a few seconds in dark before capturing the spectrum so that the dynamic process has already reached the equilibrium. In the beginning, the reflection band was centered at 1.35 μm as a result of right-handed circular polarized light being reflected. Upon UV exposure, the

#244290 Received 2 Jul 2015; revised 15 Aug 2015; accepted 17 Aug 2015; published 19 Aug 2015

isomerization took place to decrease the twisting power of PSC-01. Thus, the band shifted to a longer wavelength. Within 3 seconds, it moved out of the detectible spectral region (>2500 nm), which is limited by the employed glass substrates. However, after ~8 s of the same UV exposure, the band reappeared and moved towards a shorter wavelength. Although these reflection bands seemed similar to previous ones, by using a polarized light source we identified that they had an opposite handedness. After 22 s, the band stopped shifting and its center rested at around 1.45 μm. Note that in the longer wavelength region, the corresponding pitch length is longer. That means, fewer pitches exist in the CLC cell because the cell gap is fixed. As a result, the peak reflectance is slightly lower but the bandwidth is wider. From Fig. 5, the reflectance is ~30%. To enhance the reflectance in IR region, we can use a thicker CLC layer, but the tradeoffs are longer reaction time and increased defects due to weaker surface anchoring.

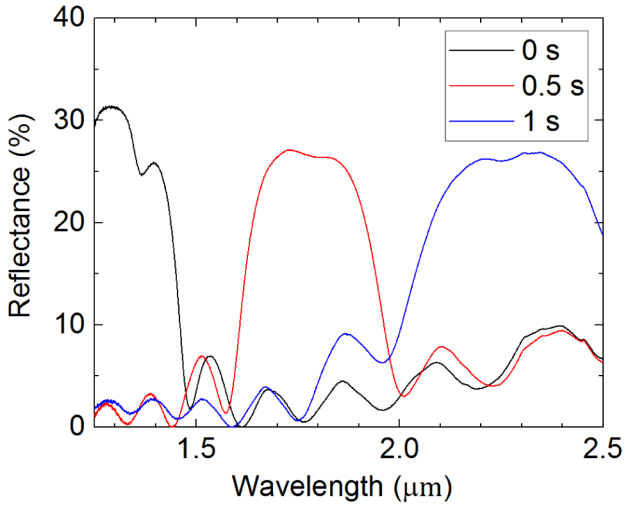

Fig. 4. The reflection band of the sample under 15.5-mW/cm^2 UV exposure rapidly shifts toward a longer wavelength region. The lower end and higher end of detection limit is determined by the spectrometer and the glass substrates, respectively. As confirmed with a polarized light source, the reflected light was right-handed.

#244290 Received 2 Jul 2015; revised 15 Aug 2015; accepted 17 Aug 2015; published 19 Aug 2015

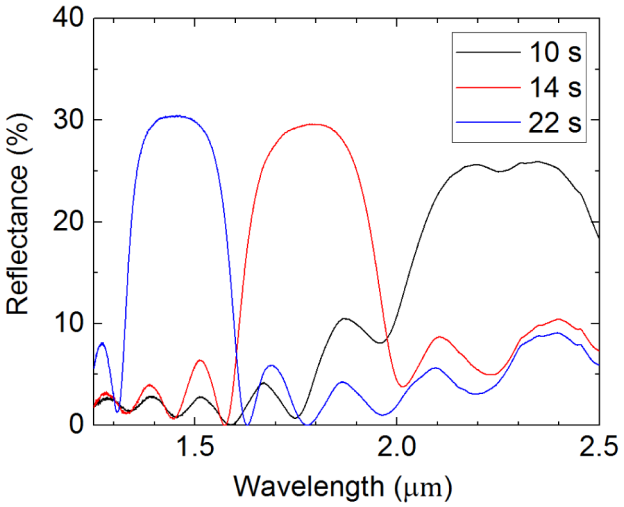

Fig. 5. After 10 s, the reflection band of the sample shown in Fig. 4 reappears from the longer wavelength side and gradually shifts toward the shorter wavelength side. Although the reflection band seems similar, its handedness is actually opposite.

We plot the inverse of the center wavelength with respect to exposure time in Fig. 6 with the right-handed band being positive and the left-handed one being negative. Due to the limited detection power, no data points were accessible in the long wavelength region. We observed an exponential decay.

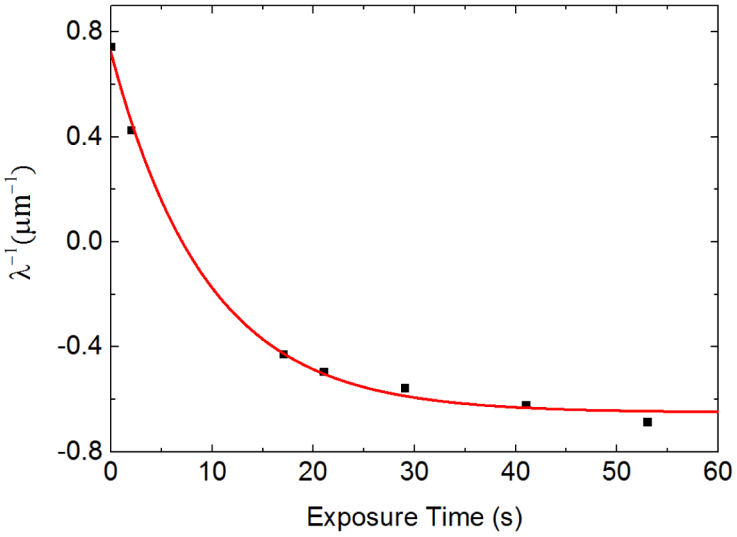

Fig. 6. The inverse of the wavelength with respect to UV exposure time shows an exponential decay trend. The data agrees well with the fitted curve using Eq. (5).

This trend can be modeled by considering the *cis*- and *trans*-isomer concentration being C_c and C_t, respectively, and the concentration of photo-stable chiral material being C_n. Let the helical twisting power respectively be β_c, β_t and β_n. Therefore, we can obtain a relation for exposure time and center wavelength [25]:

$$\lambda_0 = n / (C_c\beta_c + C_t\beta_t - C_n\beta_n). \quad (2)$$

#244290 Received 2 Jul 2015; revised 15 Aug 2015; accepted 17 Aug 2015; published 19 Aug 2015

The minus sign in Eq. (2) accounts for the left-handedness of the non-azo-chiral material. Under static UV illumination, C_t decreases exponentially while C_c increases complementarily, that is:

$$C_t = C_{c0} e^{-t/\tau}, \tag{3}$$

$$C_c = C_{c0}(1 - e^{-t/\tau}). \tag{4}$$

Here C_{t0} is the concentration of *trans*-isomer at t = 0 and τ is the isomerization time constant. Plugging Eq. (3) and Eq. (4) into Eq. (2), after some algebra we obtain the following relation:

$$\lambda_0^{-1} = (C_{t0} e^{-t/\tau}(\beta_t - \beta_c) + C_{t0}\beta_c - C_n\beta_n)/n. \tag{5}$$

In Eq. (5), there are four fitting parameters, β_c, β_t, β_n, and τ. In order to validate the fitting accuracy, we cross-check the first three parameters, β_c, β_t and β_n, through Eq. (2) using the samples with only one chiral dopant, i.e. samples with C_{t0} or $C_n = 0$. Indeed the fitted result agrees well with the measured helical twisting power. We summarize the obtained results in Table 1.

From Eq. (5), in order to let the final handedness-inverted reflection appear at the same initial wavelength, i.e., $\lambda_0(t=0) = -\lambda_0(t \to \infty)$, the system should satisfy:

$$\lambda_s = 2n / C_{t0}(\beta_t - \beta_c), \tag{6}$$

where λ_s denotes the shortest achievable reflection wavelength.

Table 1. Comparison of fitted (with opposite-handed mixture, sample 1) and measured helical twisting power of *trans*-PSC-01 (β_t), *cis*-PSC-01 (β_c) and S-5011 (β_n) in BL-038. C_{c0} and C_n are the concentration of PSC-01 and S-5011, respectively.

Sample	C_{c0} (wt%)	C_n (wt%)	β_t (μm^{-1})	β_c (μm^{-1})	β_n (μm^{-1})
1	4.75	1.80	64.18	16.31	103.8
2	-	2.33	-	-	105.5
3	6.28	-	64.13	15.84	-

From Eq. (6), to shorten the reflection wavelength we should use a photo-responsive chiral dopant with high solubility and/or wide tunability in twisting power. With $\beta_t - \beta_c$ = 47.87 μm^{-1} and n = 1.65, we plotted the theoretical relation between λ_s and C_{t0} (the concentration of PSC-01) in Fig. 7. From Fig. 7, if we could achieve 10wt% solubility, then we should be able to tune the reflection wavelength to the visible region. If the solubility could reach 18 wt%, then the tuning range would extend to UV region. However as Fig. 1 shows, the solubility of PSC-01 in BL-038 is limited to ~8 wt%.

#244290 Received 2 Jul 2015; revised 15 Aug 2015; accepted 17 Aug 2015; published 19 Aug 2015

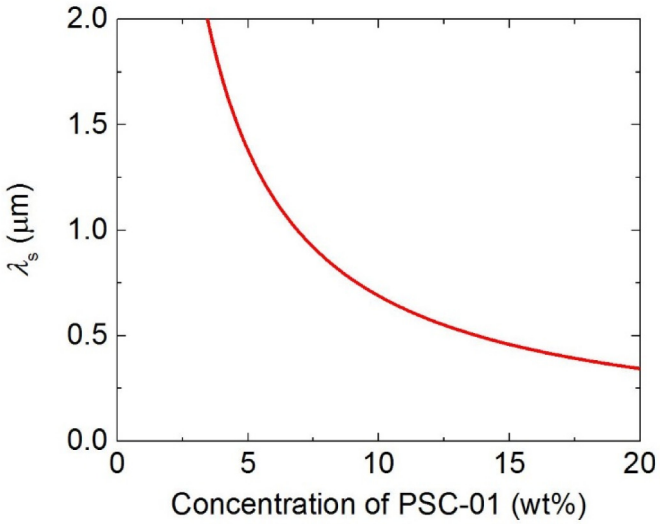

Fig. 7. The calculated λ_s through Eq. (6) vs. the concentration of PSC-01. LC host: BL-038.

To boost solubility, we could slightly increase the operation temperature [26] or modify the chiral structure. In [27], a similar chiral structure to that shown in Fig. 1 but with a longer ester cyclohexane-phenyl group, as Fig. 8 depicts, has been reported. This compound has a more flexible tail so that its solubility is expected to be higher than 10%. As a result, the tuning range should be able to extend to the visible region.

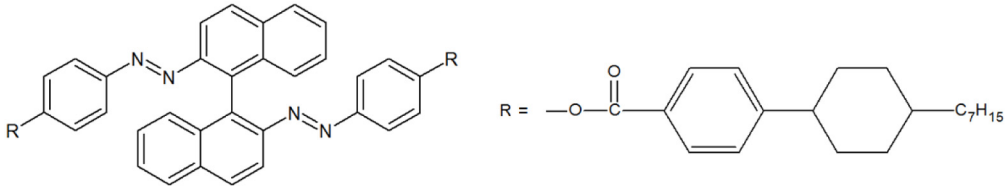

Fig. 8. A potentially high solubility photo-sensitive chiral dopant reported in [27].

Next, we examine the relation between the tuning time constant (τ) shown in Eq. (5) and the UV intensity. Figure 9 shows that with increased UV intensity, the tuning time constant decreases linearly as the UV intensity increases. As the intensity increases from 8.2 mW/cm^2 to 15.5 mW/cm^2, τ decreases to nearly half of its original value. This linear relationship can be understood since the photo-chemical reaction probability is the same for each photon, while the intensity is proportional to the number of photons. This enables us to either increase or decrease the tuning speed based on different needs.

Finally, as demonstrated in Fig. 10, it is possible to pattern different chirality regions on a single substrate through a photomask with repetitively left- and right-handedness strips at a resolution of 50 μm, roughly the pixel size of a smartphone. The random lines in each strip are oily streaks found in a cholesteric sample [28]. With this property, one can create films with versatile properties for new photonic applications.

#244290 Received 2 Jul 2015; revised 15 Aug 2015; accepted 17 Aug 2015; published 19 Aug 2015

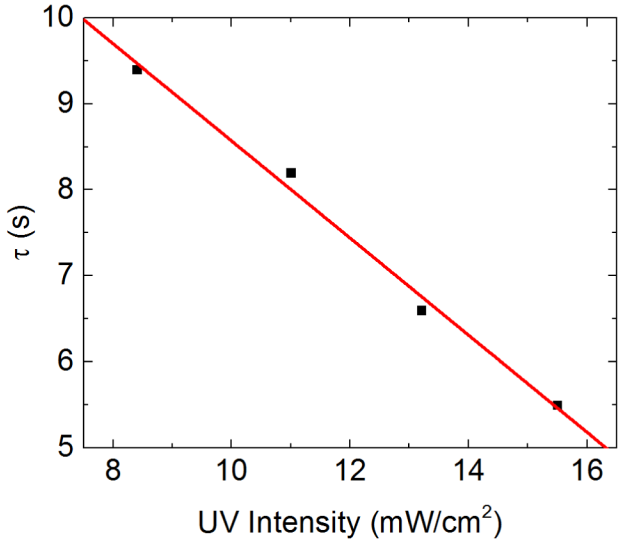

Fig. 9. The reaction time constant decreases linearly as the UV intensity increases.

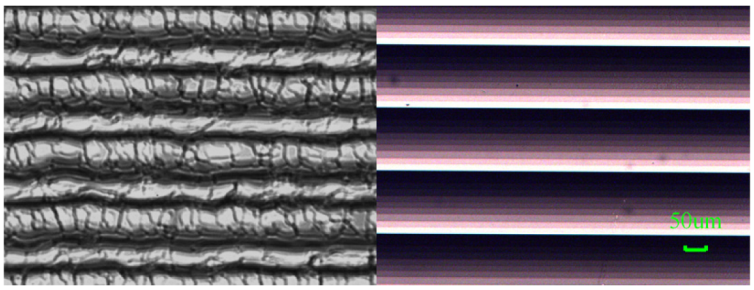

Fig. 10. The sample exposed with UV light (left) through a photomask (right). The two different repeating regions correspond to the right- and left-handed helix from top to button. The random lines in the sample are the oily streaks that occur in a typical cholesteric sample.

4. Conclusion

We have shown that with a highly soluble photo-sensitive chiral dopant, one can easily obtain chirality inversion of selective reflection in cholesteric liquid crystals. A wide tuning range is obtained and the selective reflection can be tailored from left-hand to right-hand. If a photo-sensitive chiral dopant with even higher solubility is used, the tuning range could reach visible or UV region by properly controlling the dopant concentration. The tuning time can be shortened by increasing UV intensity or decreasing cell gap; the latter approach has a tradeoff in lower reflectivity. Finally, we also showed how to obtain patterned or pixelated photo-tunable CLC device for broader photonic applications.

Acknowledgments

The UCF group is indebted to AFOSR for financial support under contract No. FA9550-14-1-0279. The PKU group gratefully thanks for financial support under Grant no. 2013DFB50340 from The Major Project of International Cooperation of the Ministry of Science and Technology.

#244290 Received 2 Jul 2015; revised 15 Aug 2015; accepted 17 Aug 2015; published 19 Aug 2015